A Study of the Mechanisms Involved in Friction Welding of Aluminum Alloys

During high-speed sliding under high axial pressures, severe wear and subsurface circumferential flow occur during the rising part of the torque curve

BY M. RAO AND T. H. HAZLETT

ABSTRACT. Much has been written since the original work was published by Vill and co-workers in Russia regarding friction welding as a bonding process, and numerous attempts have been made to explain the actual mechanism involved in this complex process. The changing progressive stages of the interactions involved are a function of the instantaneous mechanical, physical, and adhesion properties of the contacting surfaces and of the mechanical and physical properties of the solids beneath the surfaces.

As the rate of sliding is increased, high temperatures are reached due to high rates of plastic deformation which in turn affect the properties of both the surfaces and of the underlying metal. The consequent change in properties in the sliding members will in turn lead to progressive changes in the interactions involved. An abundance of already-recorded experimental data clearly demonstrate that the adhesion characteristics of the sliding metal couple play an important role in friction resistance, but there are differing views as to the mechanism involved. The study reported herein is an attempt to more clearly define the actual progressive mechanisms as they change during the friction welding of 7075-T6 aluminum alloy.

Previously described equipment was modified to permit a variable speed range from 800 to 4500 rpm. Transmission of the rotation from the 7.5 hp motor, to the rotating specimen is made through an electromagnetic clutch which is designed to disengage the inertia of the motor-gear system when the rotating specimen is suddenly stopped at any predetermined point in the welding process. Simultaneous records were made of the instantaneous torque, axial pressure, axial shortening (upset) and speed.

Considerable detail was given to studying the torsional displacements since these strains constitute an important factor in the bonding resistance that is created. Torsional strains at and behind the interfaces are created by the transmission of torques through the semicontinuous interface. Unique experiments were devised to study the progression of these torsional strains as the welding process proceeded.

The effects of the independent variables of speed and axial pressure were studied in detail, and their influence on the mechanism is described. Studies with the electron scanning microscope were invaluable in analyzing the initial breakdown of the surfaces.

In general it was found that during the high-speed sliding under high axial pressures, severe wear and subsurface circumferential flow occurred during the rising part of the torque curve. Further, tensile stresses created during the release of intermittent loads on the surfaces were noted, and the intimate contact of nascent surfaces appears to be the principle mechanism of formation of adhesion bonds with consequent wedge formation and mass disruption of the contaminated surfaces.

The top of the torque curve represents the stage at which subsurface flow is initiated over the entire cross-section of the specimens. Further, it was found that there was a unique upset for a given speed and axial pressue at which thermal recovery processes dominate over the strain rate effect. Higher speeds for a given axial pressure lower this unique upset value. Weld strengths did not increase appreciably with welding times beyond this point.

It was found that more heat was conducted into the stationery specimen than into the rotating member, since part of the heat is emitted into the atmosphere from the rotating specimen due to convection. For the same speed and lower axial pressures, flash formation became more dependent on the temperatures reached in the subsurfaces, thereby satisfying an "effective flow-stress" criterion which decreased with increasing temperature. The upset rate was, therefore, more time-temperature dependent and lower for lower axial pressures. Further, there was evidence of the pressure dependence of the creation of the vicso-plastic region at high temperatures near the interface.

M. RAO is with the Technical Staff, Bell Telephone Laboratories, Indianapolis, Ind., and T. H. Hazlett is Professor of Mechanical Engineering, University of California, Berkeley, Calif.

Paper to be presented at the AWS 51st Annual Meeting in Cleveland, Ohio, during April 20-24, 1970.

Introduction

This investigation was carried out to study the non-steady state of progressive frictional interactions that take place during the conventional friction welding of aluminum alloy 7075-T6. Attention was focused on some of the important phenomena that occur during this frictional sliding process under different conditions of rotational speed, axial pressure and at different progressive stages from shortly after contact till a substantial flash deformation and welding was obtained for one-half inch diameter couples.

This type of study requires an understanding of the interactions that take place when the sliding members are in contact under a normal load (axial pressure) and the force parallel to these surfaces (torque) which resist the relative movement of the two surfaces. The changing progressive stages of the interactions involved are a function of the instantaneous mechanical, physical and adhesion properties of the actual contacting surfaces and of the mechanical and physical properties of the metal beneath these surfaces.

The contacting surfaces of the two members being welded have a finite roughness and the state of these surfaces is a function of the process used to create them, e.g., turned, rolled, ground, cast, etc. A thin work-hardened layer at the surface is generally formed by the prior processing.

The work-hardened state of the surface layers and the geometry of the surface topography are known to affect the initial sliding interactions.[1] These surfaces are also generally reactive to environmental contaminants such as oxides, lubricants, water vapor, etc.

Properties of the thin films formed by environmental conditions are different from those of the base metal, and the consequent discontinuity between these films and the base metal affect the progress of the sliding interactions.[2] As the rate of sliding is increased, high temperatures are produced at the contacting surfaces due to the high rates of plastic deformation. The resulting temperatures, in turn, affect the properties of not only the surfaces in contact but also those of the underlying metal. These continuous changes of properties will lead to progressive changes in the interactions between the two contacting surfaces.

The current study is concerned with the type of sliding process in which both surfaces are in continuous repetitive contact, and the emphasis of the investigation was on the mechanism of the plastic deformation and subsequent metallurgical bonding of the two contacting surfaces.

Nature of the Friction Interactions

Sliding resistance under high normal pressures is very complex, and the total frictional resistance during initial sliding is a summation of the resistances of each individual contacting region between the asperities on the two surfaces. As sliding progresses, the number of individual contact regions increase. Accordingly, there will be interactions not only between the asperities of the two surfaces, but also between neighboring regions on the same surface to accommodate the plastic displacements that occur.

If the resistance to sliding of the contacting regions is sufficiently high, plastic flow will be initiated in the substrate when a yield criterion, based on the properties of the base metal, is satisfied. The yield criterion at temperatures above 0.4 to 0.5 of the absolute melting point for most metals requires a relatively low effective flow-stress. Steep thermal gradients normal to the interacting surfaces restrict plastic deformation in the substrate layers to a very narrow region.

Interactions that take place due to the tendency of the surfaces to form strong bonds which are not destroyed when external loading is removed are defined as adhesion. There is an abundance of experimental data which indicate that the adhesion characteristics of the sliding couple play an important role in sliding frictional resistance, but there are differing views as to the mechanisms involved. Bowden and Tabor[3] have accounted for frictional resistance as being due to forces required to overcome the shear strength of the adhesion junctions formed, without any emphasis on the contribution of bulk deformation. Kragelskii,[4] on the other hand, emphasizes the forces required for bulk deformation of the subsurface metal with the contention that good adhesion characteristics of the couple increases the resistance to bulk deformation, thereby involving a large volume of plastically deformed metal.

A study of wedge formations during sliding by Cocks[5] and similar studies by Antler[6] and Anbinder and Prances[7] indicate that the resistance to overcome strong adhesive bonds under conditions of severe friction is caused not so much by the shearing of the bonds themselves. It is instead caused by the bulk deformation of the wedges formed ahead of the bonding regions in the direction of the relative velocities on the surfaces and also by the sublayer shear at the base of these wedges.

The relatively severe conditions studied in this investigation produce adhesion junctions sufficiently great for plastic flow to start in the softer sublayers, thereby accommodating the motion of the strong interfacial adhesion junctions without shearing during sliding. High temperatures also result very rapidly due to the high rates of plastic deformation. This affects the frictional interactions and contributes to prolonging the nonsteady state condition. This continues until the rates of heat generation caused by plastic flow in the repetitive contact sliding system is balanced by the resulting heat dissipation.

Very little work has been done in studying the progressive stages of the friction welding process in terms of

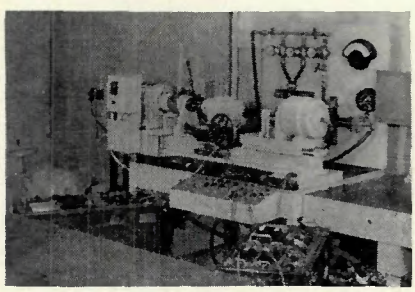

Fig. 1—General view of equipment and recorders

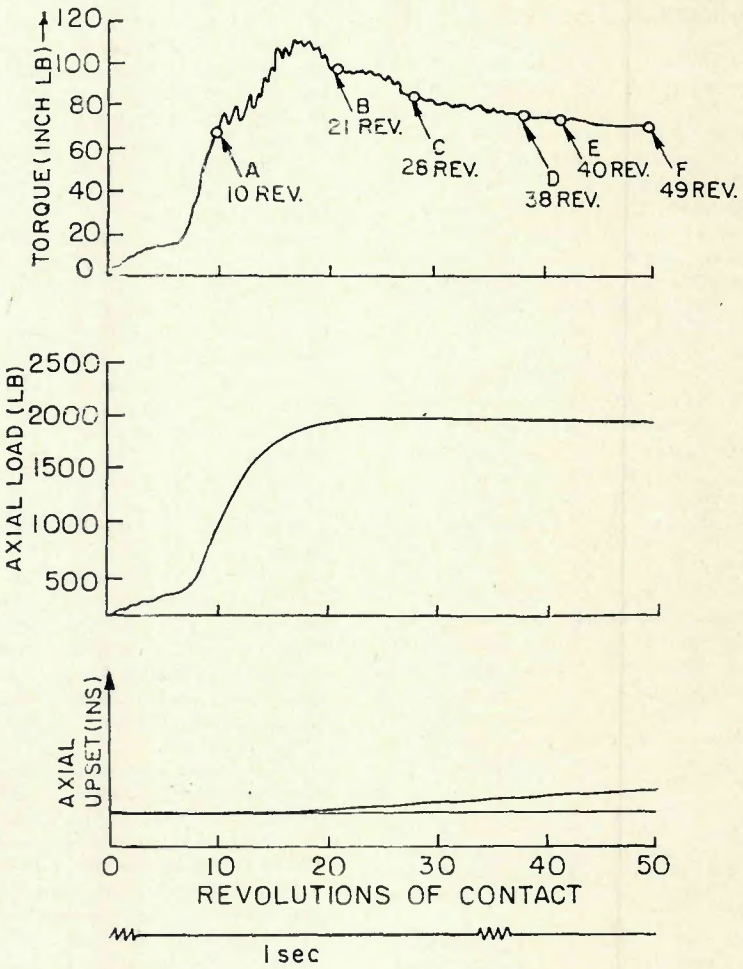

Fig. 2—Aluminum 7075-T6 1/2 diam specimens—2000 rpm, 2000 lb axial load

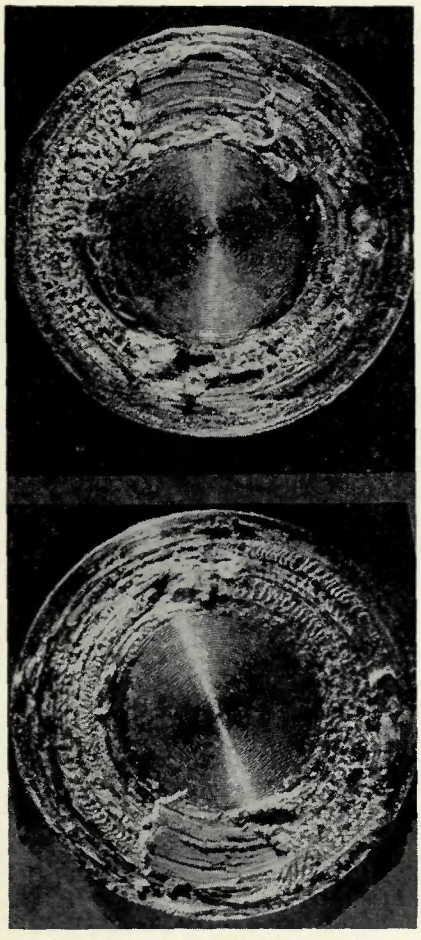

Fig. 3—Wear of contacting surfaces in the rising portion of the torque curve. A (top)—non-rotating specimen (7076-T6 aluminum, 2000 rpm, 10,000 psi axial press, 10 revs. of contact); B (bottom)—rotating specimen (counter-clockwise direction of rotation)

the surface interactions and the resulting plastic deformation for different conditions of speed and axial pressures. Most investigators have been concerned with obtaining the highest strength bonds possible for different metal combinations by the trial-and-error approach.

Inferences as to the interactions involved from sectioned and etched specimens at different stages of the bonding process have not been fully utilized in attempting to understand the surface interactions and of the bulk plastic deformations that occur. Hasui et al[8] are among the few investigators who have used this technique to make inferences regarding the temperatures reached in the vicinity of the welds for dissimilar metal bonding. Hasui and his coworkers have also utilized the extrapolation of thermocouple data to determine maximum interface temperatures.

Weiss and Hazlett[9] have measured average temperatures for dissimilar metals using the Seebeck effect. These studies indicated that the average temperature at the interface was well below the melting point of the metals of the dissimilar couples involved or their potential phases. Hasui, on the other hand, concluded that there was a high probability that a molten phase developed in certain regions near the periphery of cylindrical specimens during frictional heating. There is no method available to date to accurately measure temperatures in the minute localized regions of sliding contact under friction welding conditions.

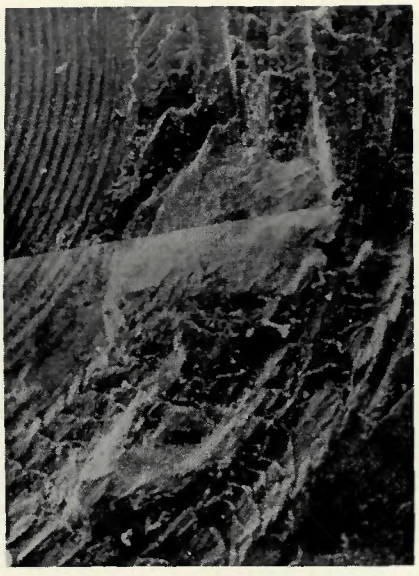

Fig. 4—Wedge formation—3500 rpm, 10,000 psi axial pressure, 10 revolutions of contact. X28 (reduced 33% on reproduction)

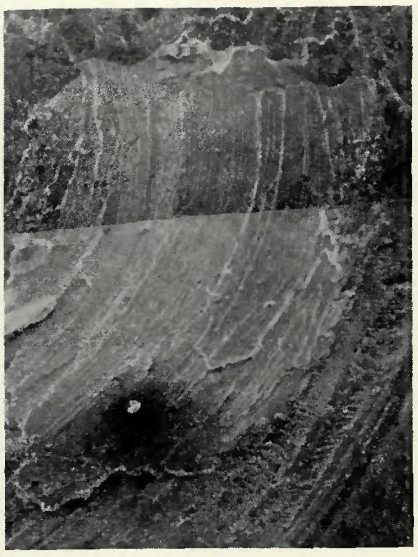

Fig. 5—Smearing of wedge—3500 rpm, 10,000 psi axial pressure, 10 revolutions of contact. X28 (reduced 33% on reproduction)

Equipment

The friction welding equipment previously used in this laboratory was rather drastically modified for the present study. The present equipment is shown in Fig. 1. A 7.5 hp variable speed-drive motor was utilized to provide power for the rotating specimen. This change together with an added provision for changing the gearing ratio between the drive motor and the spindle permitted selection of any given speed from 800 to 4500 rpm. Transmission of power from the motor to the rotating specimen was made through an electromagnetic clutch and a positive pulley belt system. The clutch is provided to disengage the large inertia of the motor gear system when the rotating specimen is suddenly stopped at the end of the process. An additional essential feature of the control system permitted stopping the weld cycle at any predetermined number of rotations of the specimen.

As in the past, instantaneous torque and the applied axial pressure on the specimen were measured independently and the speed of rotation was recorded directly from the output voltage of an electromagnetic tachometer which was directly coupled to the rotating shaft. The specimen could be brought to a stop in 6 to 7 revolutions at rotational speeds of 3500 rpm while at 1000 rpm the response was 1 to 2 revolutions.

Experimental Procedure

All of the work described herein was carried out on 7075-T6 aluminum alloy, $^1/_2$ in. in diameter and 3.5 in. long. These specimens themselves extended $^5/_{16}$ in. beyond the holding collets for both members.

Contacting surfaces for all specimens were prepared by taking the last five facing passes on the lathe in the sequence of feeds of 0.005 in./revolution followed by 3 passes of 0.0021 in./revolution with a depth of cut of 0.001 in. for each pass. This procedure was used to obtain a similar geometrical surface topography with minimum work-hardening of the surfaces. All machining of the contacting surfaces was made without any lubrication, and the only precaution taken was to perform the experiments within 24 hours after the specimens were prepared.

Split Surface Specimens

The standard procedure of examining microstructures after a certain stage of progression of the welding process has heretofore been to section the welded specimens through a meridian (i.e., center) of the specimen and to make qualitative inferences from observations of the polished and etched surfaces. Such observations have been very helpful but do not reveal any information concerning

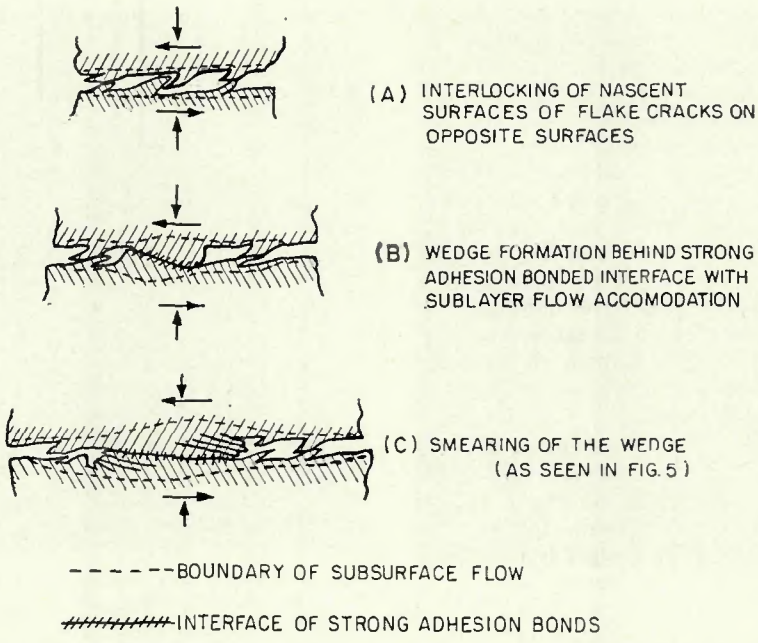

Fig. 6—Progressive stages of mass disruption of the surfaces in the rising part of the torque curve

torsional displacements. The torsional strains constitute an important factor since such strains behind the interface must be created by transmission of torque through the semi-continuous interface.

Lines scribed in the axial direction on the outer surfaces of the cylindrical specimens before welding is initiated will indicate torsional displacements of the peripheral elements after start of welding. Experiments, however, showed that attempts to draw inferences about torsional flow of the internal sections from these peripheral torsional displacements can be erroneous.

In an attempt to overcome this deficiency, split cylindrical specimens having the split through the meridian plane were used. The use of such specimens has been well established in axi-symmetric extrusion of metals by Kobayashi and Thomsen.[10] The split specimen may behave identically to a full specimen, without separating about the meridian plane during the large torsional strains. Also, the recorded feedback parameters of torque, axial shortening, etc. may be idential. When these conditions are encountered the displacement of the split plane in the torsional and radial directions at different cross-sections may be assumed to be the same as the displacements of a hypothetical plane in solid specimens; moreover, such specimens can be considered as consisting of an infinite number of meridan planes.

For reasons of symmetry and continuity, all points at the same radius for a given cross-section at right angles to the axis of the specimen will have displacements identical to this split plane. After bonding, sections at right angles to the axis of the welded specimens, taken at varying distances behind the interface will show a deformed line displaying the torsional distortion plane for that section. Except where excessive deformation and high temperatures cause a continuous region across the split surface, torque and speed measurements from experiments showed that the split specimens behaved in an identical manner to a solid specimen, without separating if the specimens extended beyond the collets by $^{5}/_{16}$ in. or less.

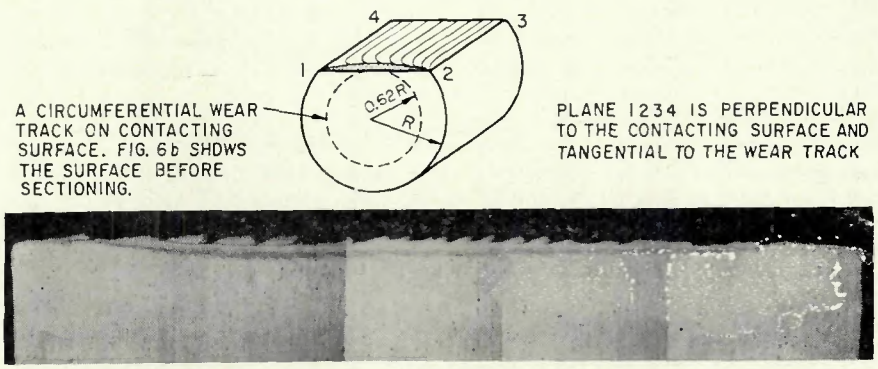

Fig. 7—Effect of high speed sliding on the subsurface region during the rising part of the torque curve. A (top)—sketch; B (bottom)—photomicrograph of polished and etched plane 1234. X22 (reduced 50% on reproduction)

Rising Portion of Torque Curve

The mechanism of the breakdown of the contacting surfaces during the rising portion of the torque curve was studied from runs made at 2000 rpm and 10,000 psi. The points of cutoff were chosen to stop rotation in the rising portion of the torque curve. The resulting surfaces were observed under a low power microscope to obtain information as to the nature of the surface interactions.

One specimen from this series, which was stopped after 10 revolutions where a strongly adhering bond had not yet occurred, was used to determine the effect of the interactions at the interface and in the sublayers of the specimen for such a short progression. The contacting surface was examined and the rotating half of the specimen was then sectioned on a plane at right angles to the friction surface at a radial distance of 0.155 in. from the center. This sectioned plane was approximately tangential to a "wear track" which is a circumferential segment on the worn surface of the specimen. Sections through the meridian plane would have been approximately 90 deg to a wear track and would not have revealed the large torsional shear displacements that take place in the subsurface. The specimen section mentioned above, however, gave an indication of the large plastic shear strains in the subsurfaces.

Progressive stages of the nonsteady state interactions under preset speed and axial pressures were studied by examining the microstructures of polished and etched meridian planes of specimens which had been in rotational contact for increasing numbers of revolutions. The initial series of such runs were performed at speeds of 3500, 2000, and 1000 rpm with an axial load of 2,000 lb. (10,000 psi for $^{1}/_{2}$ in. specimens).

The effect of varying the axial pressure on the progression of the welds with microstructures was studied at the speed of 3500 rpm only. Runs were made for two different progression points at pressures of 5,000 psi, one at the top of the torque curve and another at an upset of 0.035 inches which was well beyond this stage. Other runs were made at 1,000 and

2,500 rpm, at 5,000 psi axial pressure with an upset of 0.035 inches for which records of torque, axial pressure and upset were compared.

Results and Discussion

Since the rotational speeds in this study were in the range of 1,000 to 3,500 rpm on $^1/_2$ in. diameter specimens, sliding speeds of the order of 5 to 80 in./sec were achieved. At these high speeds even a few revolutions of contact can raise the temperature at localized spots on the surfaces to a relatively high value. Cylindrical solid specimens experience complex distribution of axial pressures, torsional stresses and temperatures across the interface, all of which are factors that cannot be easily evaluated either experimentally or analytically.

A plot of the three easily measurable parameters for a typical weld is shown in Fig. 2. These are torque, axial load and axial upset. Of the three, the top curve (torque) is probably the most significant and will be used as a basis for the discussions in the remainder of this paper.

Mechanism of Surface Breakdown in the Rising Portion of the Torque Curve

Figure 3 is a photomacrograph of the specimen in the rising portion of the torque curve at point "A" of Fig. 2. The two mating surfaces are shown after separation. Typically, the central portion of the specimen did not experience significant axial loading at this early stage. This may be caused by slight unevenness of alignment of the contacting surfaces. This lack of plastic flow in the center is characteristic for all specimens produced under all variables investigated during the rising portion of the torque curve. Figure 3 also shows a few wedges and a relatively large smeared region, whereas the major area of the wear tracks are irregular in appearance at this magnification. The differences in these areas are more clearly illustrated in Fig. 4 and 5 which show wedge type formation as well as smearing of the wedge.

A representation of the progressive mechanisms of the interlocking is shown schematically in Fig. 6. Wedge formation and growth, followed by smearing of the wedges is illustrated. The formation and smearing stages on one of the surfaces are shown in Fig. 5 and 6. Since aluminum oxides form a very tenacious oxide film, it is difficult to conceive of the disruption of this film by any other mechanism unless very large deformations were achieved. Very large deformations can cause the subsurfaces to become sufficiently viscous to disrupt the oxides, thereby exposing nascent metal surfaces. Aluminum oxide films have a melting point much higher than the base metal, and temperatures generated due to sliding are not sufficient to disrupt this layer by temperature alone.

Subsurface flow for the specimen shown in Fig. 3 is illustrated in Fig. 7 on a plane tangential to the wear track at a distance of 0.62 R from the center. This micrograph shows large subsurface flow well below the surface. The long axially orientally grains flowed with a sharp right angle motion to become parallel to the contacting surfaces. This is accompanied by a disintegration of the long grains to a very fine and uniform grain structure in the region just below the contacting surface.

It may also be seen from Fig. 7 that the depth of the subsurface flow was markedly reduced in a region close to the outer radius of the specimen. This fine grain structure must be attributed to the severe amount of work and the high temperatures reached in this region. It is therefore an extremely fine recrystallized structure.

As mentioned earlier, heat generated in the early portion of the sliding process is caused by the high rates of plastic deformation of the asperities on the surfaces which come into contact. The rate of heat generated is larger than the rate of heat flow, thereby causing an adiabatic increase in temperature. Since the heat source is localized to regions where surface activity takes place, the thermal gradients in the substrate were very steep.

Despite the nonuniform surface interactions, the subsurface flow that resulted from any specific cycle of speed, nominal axial pressure, and number of revolutions was quite reproducible. This subsurface flow de-

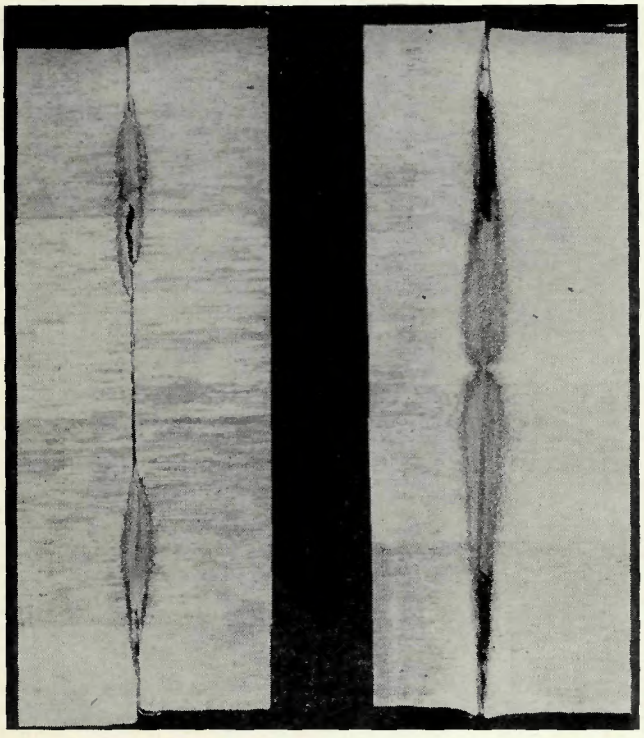

Fig. 8—Progressive stages of sliding lense formation. X11 (reduced 43% on reproduction)

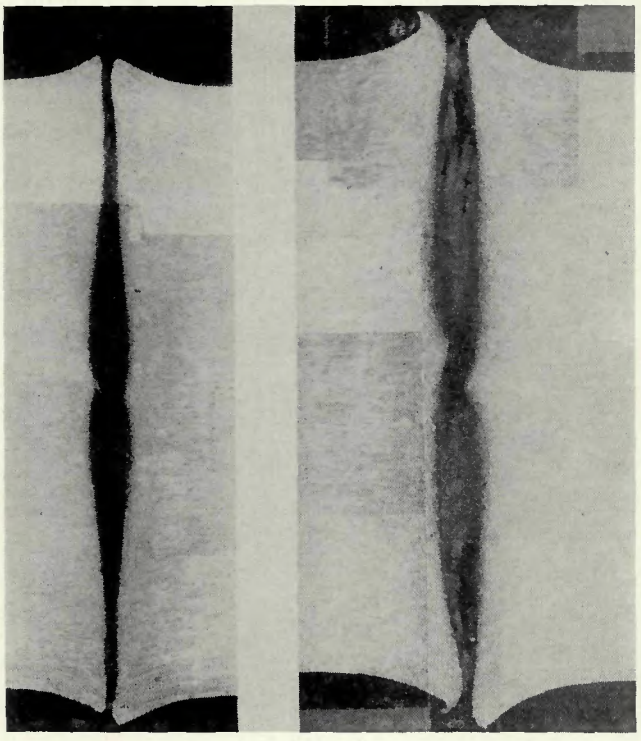

Fig. 9—Effect of rotational speed on temperature distribution (2000 lb axial load). A (left)—3500 rpm; B (right)—1000 rpm

veloped with characteristic lens shape regions as shown in Fig. 8. The structure within the lens was extremely fine-grained by comparison to the base metal.

The rising portion of the torque curve represents growth in interfacial contact area in the radial direction as well as subsurface plastic deformation under the wear regions as shown in Fig. 3 and 8 until the maximum torque is achieved. At the point of maximum torque, subsurface flow exists across the entire cross section; the convex lens region extending from the center to the periphery. No significant increase in diameter of the specimens at the interface or flash formation was indicated up to this point.

An axially scribed line on the outside surface of the cylindrical specimen indicated practically no torsional plastic strains at the periphery behind the interface before flash initiation. Split surface secimens confirmed this observation; however, they also show very large torsional flow in the lens region at some intermediate radius.

These observations indicate that the top of the torque curve represents a stage in the process where an effective subsurface yield criterion, based on the complex stress distribution, was achieved over the entire cross section. Axial and radial displacements were practically absent and the large displacements within the lens was due only to circumferential load induced by the surface interactions created by combined axial and torsional loading. The formation of a uniform fine structure close to the interface was indicative of the high temperatures and simultaneous high plastic strains required to cause recrystallization.

Although the specific reason for thinning of the convex lens region near the periphery cannot be clearly defined, the following explanations appear to be reasonable either by themselves or in combinations thereof:

1. Temperatures reached near the periphery due to the high circumferential speed may have been sufficiently high to cause localized thermal softening in a thin film, thereby reducing the friction and subsurface flow participation. This is supported by experiments which show increased participation nearer the periphery with slower speeds as illustrated by the photographs in Fig. 9 with the same axial pressure, at speeds of 3,500 and 1,000 rpm at a point just beyond the maximum of the torque curve.

2. A larger part of relatively low amount of localized heat generated near the periphery at this early stage may have been dissipated to the atmosphere by convection due to the high rotational speeds, thereby restricting the amount of heat conducted into the specimens and localizing the plastic deformation to a thin layer.

3. The localized deformation near the periphery may have been due to the nature of the axial pressure distribution where there is a drop near the periphery similar to the phenomena reported by Towle and Riecker.[11] Although circumferential shear strains may have been high, they would be restricted to a thin region due to low axial pressure.

Flash Formation After Achieving Maximum Torque

Flash formation is dependent on an instantaneous bulk yield criterion. The criterion is a function of the combined loading system created by the normal load and the torsional frictional resistance, the strain rates, temperatures, and temperature gradients. The temperature gradients involved are dependent upon the thermal diffusivity characteristics of the particular alloy, the rate of heat generation and the fraction of the heat that is lost to the atmosphere.

When flash formation takes place, an element in the substructure undergoes deformation subjected to the resultant of simultaneous displacements in three directions—axial, radial and circumferential.

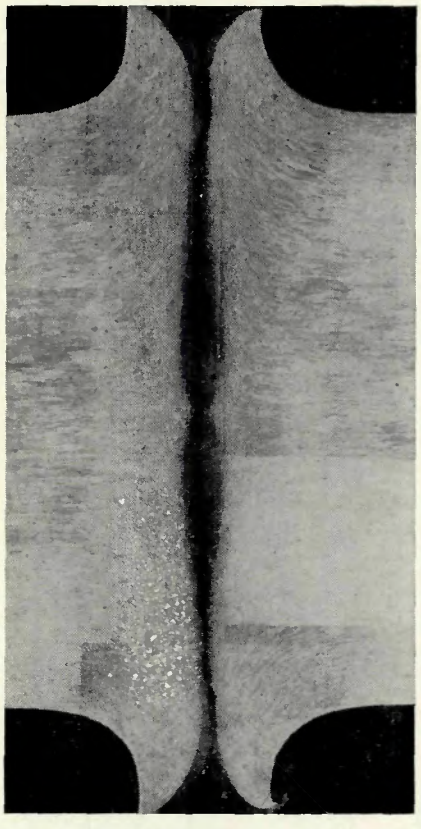

Fig. 10—Retention of lens shaped fine grained region after large deformations. X11 (reduced 42% on reproduction)

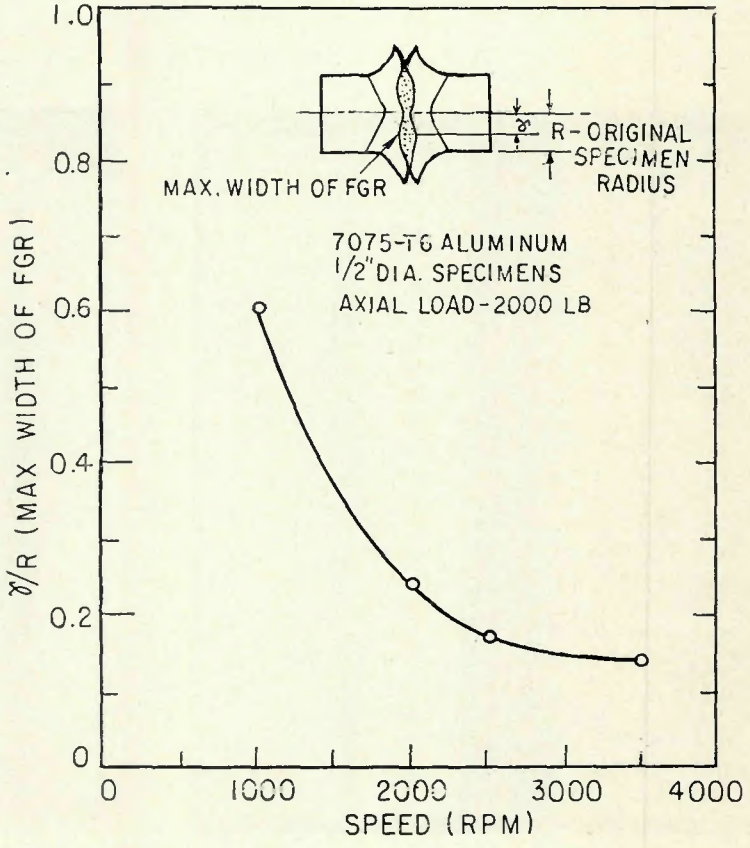

Fig. 11—Radial locations of the maximum width of the FGR lens region for different speeds

In the case of the aluminum alloy studied in this investigation, the fine grain structure in the characteristic convex lens shape was retained even up to the large deformations illustrated in Fig. 10. The deformation in this lens region is not of the conventional shear type but is subjected to high temperature visioplastic flow under large hydrostatic pressures. It must be noted that the loads were transmitted through the fine grain region to cause flow in regions behind the lens boundary.

It was further observed that once the convex lens fine grain regions formed across the entire interface, the radial location of the maximum width of the fine grain region remains stationary even after very large flash formation. Although the general shape and magnitude of maximum width of lens changed as welding progressed, the radial location of the maximum width from the center did not shift for any given speed. However, at lower speeds and the same axial pressure, the location of the maximum width moved toward the periphery but still remained at a constant location for any given speed. This is shown graphically in Fig. 11.

Comparison of Torque Curves vs. Speed for a Constant Axial Pressure

The usual plot of "torque versus time" for comparing the frictional resistance with different speeds loses sight of the variations that take place when a given number of revolutions of contact are considered at different contact velocities. Torque curves for five different speeds are plotted against the number of revolutions in Fig. 12. These curves show that, even though less time was required to reach the top of the torque curve at higher speeds, the actual number of revolutions of contact increased exponentially with increasing speeds. This is indicative of a reduced tendency to initiate subsurface flow at high speeds. The phenomenon must be intimately connected with localized thermal affects at the aspirity level of deformation which retard subsurface participation for the entire cross section.

The lower torques measured at the higher speeds, shown in Fig. 12, also indicate that the thermal affect of the high deformation rate of the asperities cause smearing with consequent early formation of nascent surfaces with a reduced tendency to wedge formation in deep subsurface plastic flow. In comparing these curves beyond the maximum torque points, the torque values drop much more steeply before reaching a steady state value as rotational speed is decreased. These observations indicate that after subsurface flow was achieved over the entire cross section at the top of the torque curve, the uneven surface interactions continued until a steady torque value was obtained. In contrast, at higher speeds, the heat generated by the asperity interactions was sufficiently high for localized thermal softening to curtail these torque fluctuations just after the peak of the torque curve was reached.

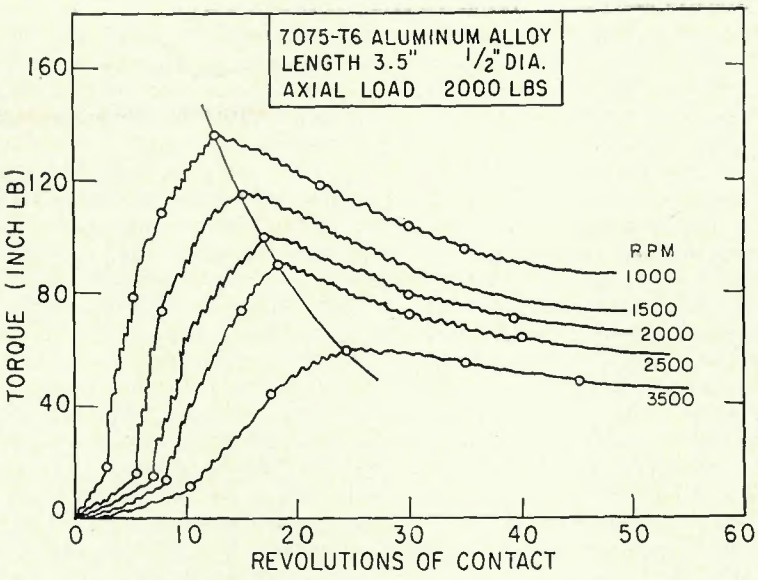

Fig. 12—Torque vs. number of revolutions of contact at different speeds (rpm) from recorder charts

Higher torque levels for a given axial pressure were always accompanied by higher rates of flash formation, because the rate of flash formation is dependent upon a combined state of stress wherein the torsional stress component is a prominent factor. This is in agreement with Von Mise's effective yield criterion where:

$$\bar{\sigma}^2 = \sigma_{zz}^2 + 3\,\tau_{z\theta}^2$$

where $\bar{\sigma}$ = effective yield stress (psi); σ_{zz} = axial pressure (psi); $\tau_{z\theta}$ = torsional stress (psi).

Since the torques were larger at slower speeds, more torsional load was transmitted to the subsurfaces

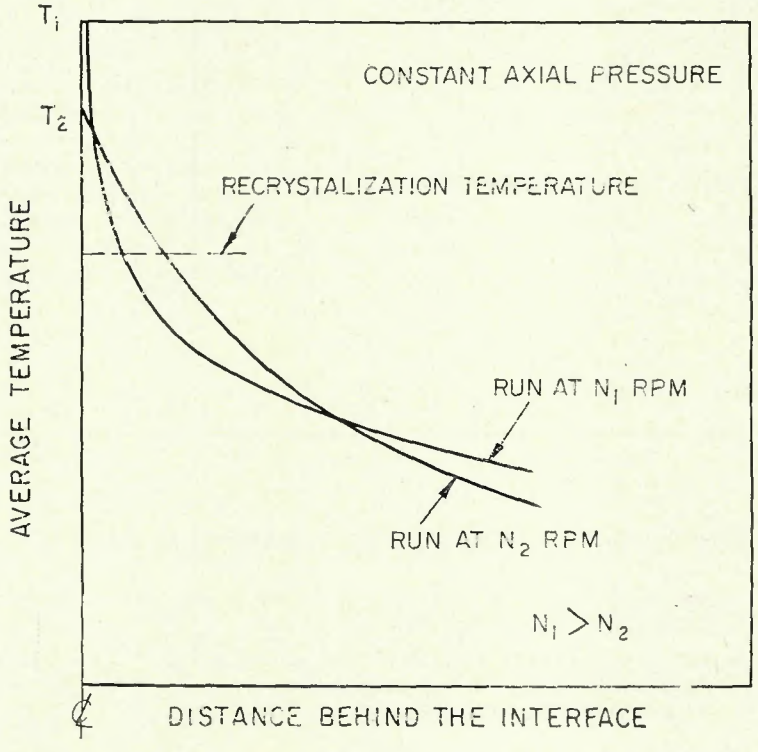

Fig. 13—Comparative hypothetical axial temperature distributions for two different speeds

thereby resulting in larger radial flow. Flash formation at higher speeds is comparatively more dependent upon the axial pressure component σ_{zz} since the torsional stress $\tau_{z\theta}$ is lower and the resulting rate of axial shortening is reduced. The distribution of radial flow was also found to be dependent upon the manner in which a varying temperature flow criterion is satisfied behind the interface.

All evidence available from this study indicated that the torsional stress component transmitted across the interface for increased rates of flash formation for a given axial pressure was largely dependent upon the absolute temperature reached and the temperature gradient behind the interface. The steeper the thermal gradient, the lower the torques transmitted to the subsurface and the lower the upset rate.

This line of reasoning leads to a comparative instantaneous temperature distribution hypothesized for different speeds as shown in Fig. 13. These hypothetical distributions show higher temperatures and steeper temperature gradients at higher speeds (N_1). The rate of upset decreases for the higher speed even though more heat may be conducted into the deeper subsurfaces to initiate plastic flow. This would be true since radial flow, contributing to upset, is more dependent upon torsional than axial loads and torques have been shown to be lower for higher speeds. At the lower speeds (N_2), however, the thermal gradient is not as steep and more torsional load can be transmitted to the surface. Figure 13 also explains how the depth of penetration of the crystallized fine grain region can be greater at the lower speeds.

Effect of Axial Pressure at 3,500 RPM

Torque increased more gradually with lower axial pressures and required a larger number of revolutions (and time) to reach the top of the torque curve. The maximum torque at 5,000 psi axial pressure was approximately 20% less than for the 10,000 psi runs.

The rates of flash propagation at the lower pressure were decreased by a time factor of approximately 3 over those at the higher pressure. This large increase in time is attributable to the fact that the effective flow stress criterion in the subsurfaces becomes more dependent on the temperatures developed in the subsurface from the heat conducted into the specimens since both the torsional and axial stresses were lower.

Since the rate of flash formation was reduced, heat generated at the interface was not removed as readily as at the higher axial pressure. Consequently higher temperatures were created near the interface.

Conclusions

1. During high speed sliding under high axial pressures, severe wear and subsurface circumferential flow occurred in the rising part of the torque curve.

2. Maximum depth of the subsurface flow was located in a region between the periphery and the center of the specimen during the rising part of the torque curve. This resulted in a convex lens region of subsurface flow.

3. The interlocking of asperities is the origin of the mechanism of initial formation of adhesion bonds which leads in turn to wedge formation and mass disruption of contaminated surfaces for aluminum alloys.

4. The top of the torque curve represents the stage where subsurface flow was initiated over the entire cross section.

5. The subsurface flow pattern after flash formation was repeatable despite variations in the initial surface condition.

6. A hypothesis that higher interface temperatures and steeper axial thermal gradients reduce torsional strain transmission at high speeds appears valid.

7. For the same speed and lower axial pressures, flash formation becomes more dependent on the temperatures reached in the subsurfaces, thereby satisfying an effective flow stress criterion which decreased with increasing temperatures. The upset rate was more time dependent and hence lower at the lower axial pressures.

References

1. Piggot, M. R., and Wilman, H., "Nature of the Wear and Friction of Mild Steel and the Effect of Surface Oxide and Sulphide Layers," Conference Lubrication and Wear, Inst. Mech. Engr., London (1957), p. 613.

2. Coffin, Jr., L. F., "Some Metallurgical Aspects of Friction and Wear," Friction and Wear Symposium Proceedings, Detroit (1957). Elsevier Publishing Co., 1959, pp. 36-66.

3. Bowden, E. P., and Tabor, D., "The Friction and Lubrication of Solids," Clarendon Press, Oxford (1954).

4. Kraghelskii, I. V., "Friction and Wear," Translated from Russian Publishers, Butterworth, Inc., Washington, D.C. (1965).

5. Cocks, M., "Shearing of Junctions Between Metal Surfaces," Wear 9 (1966), pp. 320-28.

6. Antler, M., "Processes of Metal Transfer and Wear," Wear 7 (1964), pp. 181-203.

7. Ainbinder, S. B., and Pranes, A. S., "On the Mechanism of the Formation and Destruction of Adhesion Junctions Between Bodies in Frictional Contact," Wear 9 (1966), pp. 209-227.

8. Hasui, Fukushima and Kinugawa, "Experimental Studies in Friction Welding Phenomenon," Transactions of National Research Institute of Metals, No. 4, Vol. 10 (1968), pp. 207-225.

9. Weiss, H. D., and Hazlett, T. H., "The Role of Material Properties and Interface Temperatures in Friction Welding Dissimilar Metals," ASME Metals Engineering Conference, Cleveland, Ohio (April 1966), ASME Publication No. 66-Met-8.

10. Thomsen, E. G., Yang, C. T., Kobayashi, S., "Plastic Deformation in Metal Processing," MacMillan Company, New York (1965).

11. Towle, L. C., and Riecker, R. E., "Some Consequences of the Pressure Gradients in Bridgman Anvil Devices," J. Geophysical Research, Vol. 71, No. 10 (1966), p. 2609.